

VIP Very Important Publication

Selective C–H Bond Functionalization of Unprotected Indoles by Donor-Acceptor Carbene Insertion

Juan Diego Pizarro,^a Lucía Morán-González,^{b, c} Iván González-Fernández,^a Feliu Maseras,^{b,*} Manuel R. Fructos,^{a,*} and Pedro J. Pérez^{a,*}^a Laboratorio de Catálisis Homogénea, Unidad Asociada al CSIC, CIQSO-Centro de Investigación en Química Sostenible and Departamento de Química, Universidad de Huelva, 21007 Huelva, Spain

E-mail: perez@dqcm.uhu.es; manuel.romero@dqcm.uhu.es

^b Institute of Chemical Research of Catalonia (ICIQ-CERCA), The Barcelona Institute of Science and Technology, Avda. Països Catalans, 16, 43007 Tarragona, Spain

E-mail: fmaseras@iciq.es

^c Departament de Química Física i Inorgànica, Universitat Rovira i Virgili, c/Marcel·lí Domingo s/n, 43007 Tarragona, Spain

Manuscript received: March 17, 2023; Revised manuscript received: July 2, 2023;

Version of record online: ■■, ■■

Supporting information for this article is available on the WWW under <https://doi.org/10.1002/adsc.202300252>

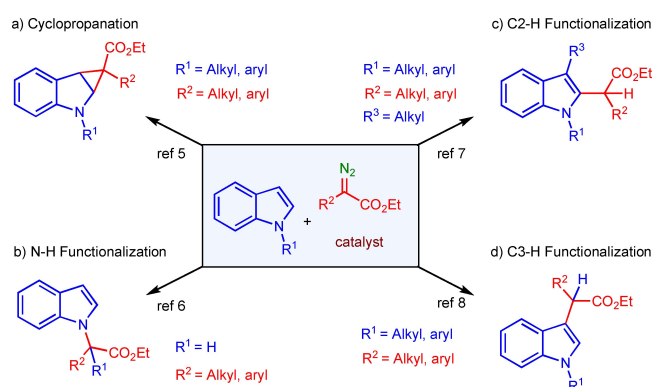
© 2023 The Authors. Advanced Synthesis & Catalysis published by Wiley-VCH GmbH. This is an open access article under the terms of the Creative Commons Attribution License, which permits use, distribution and reproduction in any medium, provided the original work is properly cited.

Abstract: Copper catalysts containing alkoxydiaminophosphine (ADAP) ligand catalyze the selective C3–H functionalization of unprotected indoles upon carbene transfer from donor-acceptor diazo compounds, the N–H bond remaining unaltered during the transformation. Mechanistic studies, including DFT calculations, allows proposing the existence of two competitive pathways, none of them occurring through the formation of cyclopropane intermediates, at variance with previously reported systems.

Keywords: Indole functionalization; carbene transfer; selective C–H functionalization; N–H bond; donor-acceptor

Introduction

The transfer of carbene units from diazo compounds catalyzed by transition metal complexes constitutes a valuable tool in organic synthesis.^[1] Among the plethora of reactions described within this methodology, the functionalization of C–H bonds upon insertion of that carbene unit is one of the most interesting targets.^[2] Its application to indole substrates has gained interest in the last decade,^[3] due to the presence of this structure in natural compounds and to their uses in the pharmaceutical and agrochemical industries.^[4] Scheme 1 shows the different examples known to date for the modification of indoles by carbene transfer reactions: (a) cyclopropanation of the C=C bond;^[5] (b) N–H functionalization;^[6] (c) C2–H functionalization^[7] and (d) C3–H functionalization.^[8] Occasionally, the six-member ring can also be



Scheme 1. Functionalization of indoles by transition metal-catalyzed carbene transfer from diazocompounds.

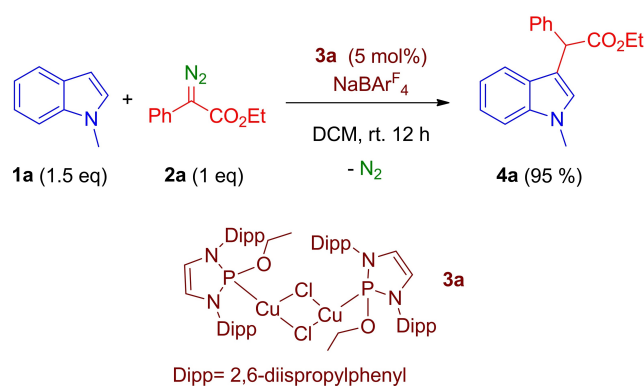
modified.^[5e] The presence of different reaction sites frequently generate selectivity issues. The preferred derivatives are those from the C2–H and C3–H sites. Most of the work toward that end has been carried out employing N-protected indoles, therefore eliminating the drawback of the N–H functionalization, which is by far the most reactive site. Systems selective for C–H bond functionalization by carbene insertion tolerant with the N–H functionality are scarce: Koenigs^[9] has described the incorporation of carbene units to C–H bonds of unprotected indoles and carbazoles, whereas Fasan and Arnold have employed more elaborated catalysts based on myoglobin or cytochrome P450, respectively, toward that end.^[10] Therefore the direct C–H bond functionalization of N–H indoles with this strategy yet constitutes a challenge in this area.

Previous work in our laboratory showed that the complexes $\text{Tp}^x\text{Cu}(\text{NCMe})$ (Tp^x = hydrotrispyrazolylborate ligand) display good catalytic properties for the functionalization of the C3–H position of protected indoles by carbene insertion from acceptor diazo compounds. However, with unprotected indoles the chemoselectivity was low, generating mixtures of products from C3–H and N–H bond functionalization.^[8b] Based on the scarcity of catalytic systems for the modification of C–H bonds of unprotected indoles, we have now targeted such goal. Herein we describe a novel family of copper catalysts containing alkoxydiaminophosphine (ADAP) ligands for the selective functionalization of unprotected indoles at the C3–H position using donor-acceptor diazo compounds, leaving the N–H group unreacted.

Results and Discussion

Initial screening. In a first attempt, N-methylindole (**1a**) and ethyl 2-phenyl diazoacetate (PhEDA, **2a**) were chosen to test the catalytic capabilities of complex $[(\text{ADAP})\text{CuCl}]_2$ (**3a**). These complexes have been previously described by our group, as well as the synthesis of the alkoxydiaminophosphine (ADAP) ligands.^[11] With a 5 mol% catalyst loading, in DCM at room temperature, and adding the diazo compound in one portion, nearly quantitative yields (> 95%) of the product formed upon insertion of the carbene group into the C3–H bond was obtained (Scheme 2). It is worth mentioning that the dinuclear nature of **3a** in the solid state is partially disintegrated in solution providing mononuclear units of composition $(\text{ADAP})\text{CuCl}$.

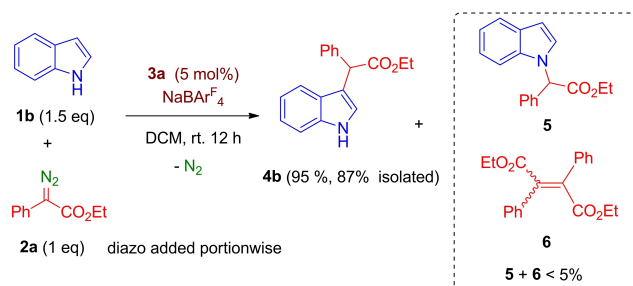
Once demonstrated the capabilities of **3a** for the insertion of carbene units into the C3–H bond, we moved to the challenging parent unprotected indole. Under the same conditions, including the addition of diazo **2a** in one portion, NMR studies with the crude extract showed a 1:1 mixture of products derived from the insertion of the carbene unit into both N–H and



Scheme 2. Functionalization of N-methylindole using $[(\text{ADAP})\text{CuCl}]_2$ as the catalyst.

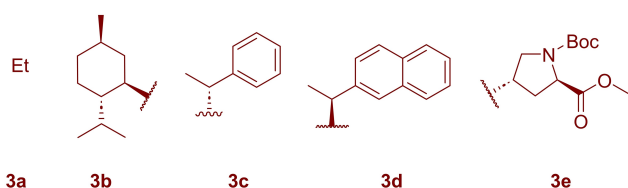
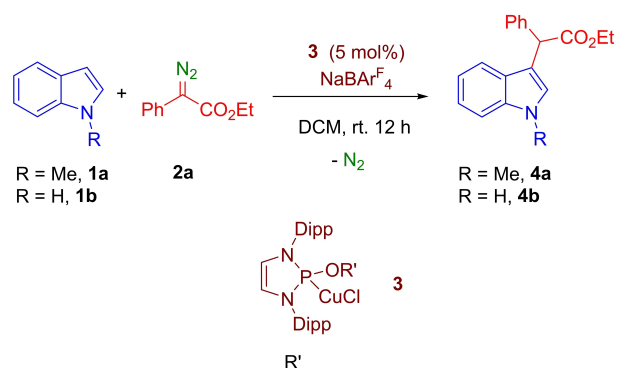
C3–H bonds (Scheme 3). Fortunately, when the same reaction was repeated with the diazo reagent being added portion-wise (7 fractions separated by 30 min each), the selective functionalization of the C3–H bond was observed, with >95% yield (diazo-based) into product **4b**, the remaining 5% corresponding to a mixture of the products of the insertion into the N–H bond (**5**) and the homocoupling of the carbene group (**6**).

Effect of the ADAP ligand. Given the availability of a family of ADAP ligands developed in our laboratory, we studied the effect of the ancillary ligand in the reaction outcome, with both N-protected and unprotected indoles **1a,b**. The results are shown in Table 1, where the nature of the R' fragment in the alkoxy group does not exert a noticeable influence in the reaction outcome: the series of five catalysts led to nearly quantitative and selective formation of the product derived from the functionalization of the C3–H bond, even for the case of the unprotected indole **1b**. Therefore, it seems that the diaminophosphine ring controls the catalytic transfer of the carbene moiety to the indole. It is worth mentioning that despite the chiral nature of the R' groups in the **3b–3e** catalysts, no significant enantioselectivity has been observed.



Scheme 3. Selective functionalization of unprotected indole at C3–H using $[(\text{ADAP})\text{CuCl}]_2$ as the catalyst.

Table 1. Study of the influence of the ligand on the reactivity of indoles functionalization.



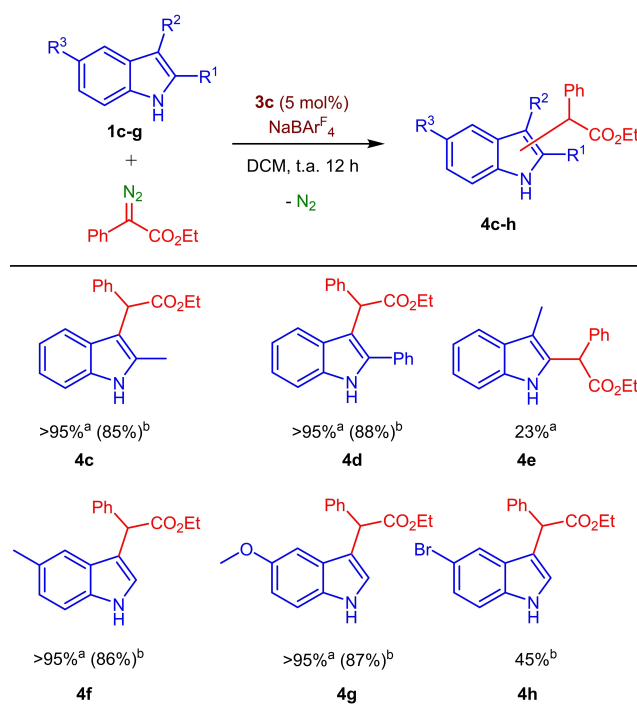
Entry	Catalyst	Yield 4a (%)	Yield 4b (%)
1	3a	> 95 ^[a] (89) ^[b]	> 95 ^[a] (87) ^[b]
2	3b	> 95 ^[a] (88) ^[b]	> 95 ^[a] (89) ^[b]
3	3c	> 95 ^[a] (89) ^[b]	> 95 ^[a] (95) ^[b]
4	3d	> 95 ^[a] (91) ^[b]	> 95 ^[a] (94) ^[b]
5	3e	> 95 ^[a] (92) ^[b]	> 95 ^[a] (91) ^[b]

^[a] ¹H NMR yield using benzaldehyde as internal standard.

^[b] Isolated yield.

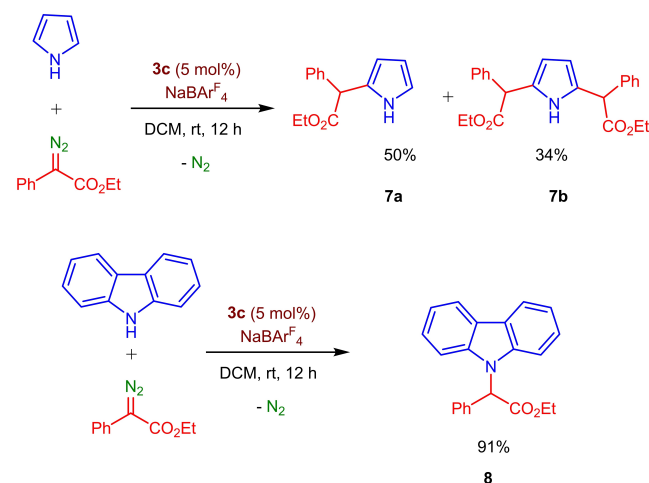
Substrate scope. To evaluate the influence of the substituents on the different positions of the unprotected indole, complex **3c** was chosen as representative catalyst. Indoles with substituted groups at C2, C3 or C5 were employed, with the results shown in Scheme 4. Substitution at C2, either with Me or Ph, led to exclusive formation of the products derived from the carbene insertion into C3–H (**4c,d**). When the substitution took place at C3, then the insertion occurred at the C2–H bond (**4e**) but only at 23% yield, the major product resulting from the functionalization of the N–H bond (**4e***, see SI). The substitution with electron-donating groups at C5 did not affect, however, the selectivity, and only modification of C3–H was observed (**4f, 4g**), with no interference of the N–H bond. Nonetheless, when placing an electron-withdrawing group at such position, selectivity was modified, and a mixture of the product of C3–H functionalization (**4h**, 45%) and that with both C3–H and N–H bonds functionalized (**4h***, 30%, see SI) was obtained.

Pyrrole and carbazole have also been tested as substrates using ethyl 2-phenyl diazoacetate as the carbene source and complex **3c** as catalyst (Scheme 5). Pyrrole underwent functionalization at the C2–H site,



^aNMR yields. ^bIsolated yields.

Scheme 4. Effect of substitution at unprotected indoles.



Scheme 5. Pyrrole and carbazole as substrates.

albeit a mixture of two products (**7a** and **7b**) derived from the mono- and di-functionalization reactions. Attempts to control the selectivity failed. It seems that once **7a** is formed, it is very reactive towards the copper-carbene intermediate to form **7b**. The use of carbazole demonstrates that when no Csp²–H bonds in the 5-member ring are available, the catalyst directs the reaction towards the N–H site, leading to compound **8** in 91% yield.

Deuteration experiments. In previous work from our laboratory, we observed the formation of cyclopropane intermediates in the reaction of indoles with diazo compounds catalyzed by Tp^xCu cores, which underwent ring opening in an acid-catalyzed process leading to the formal insertion products (Scheme 6a). Adventitious water served as proton shuttle for the formation of the C3-substituted product which therefore did not originate by a direct insertion of the metallocarbene into the C–H bond. At variance with those results, the ADAP-based system does not

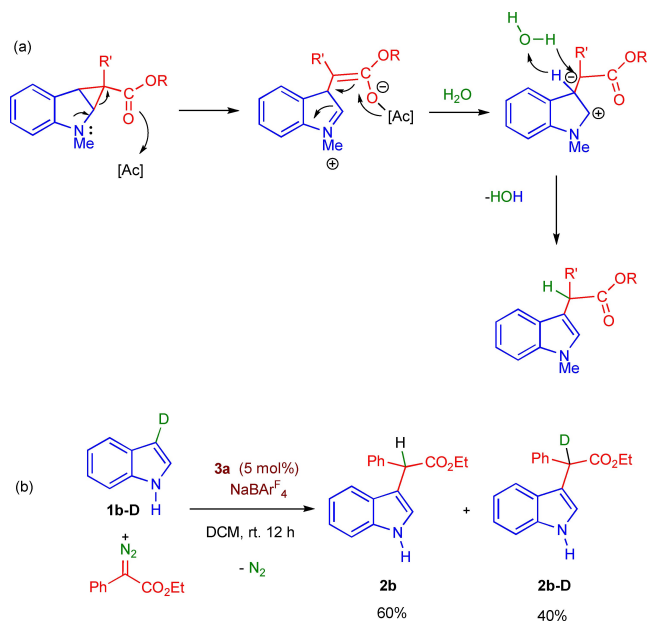
generate cyclopropanes or if they are formed, they cannot be detected in the reaction mixture.

To gather information about the mechanism, we prepared indole deuterated at C3 (**1b-D**). In this case, a 40:60 mixture of the protio- and deuterio- derivatives **2b** and **2b-D** was obtained, respectively. The incorporation of deuterium was assessed by the observance of the corresponding resonances in the ^2H NMR spectrum (Scheme 6b, Figure 1) as well as for the decrease of the integral of the $-\text{C}(\text{H})\text{PhCO}_2\text{Et}$, that provided the exact amount of incorporation. Some **1-N-D** product was also observed: blank experiments with the catalyst and D_2O in the absence of diazo compound showed that the copper complex promoted the N–D exchange, albeit no N–D insertion product was observed in the catalytic experiments. The observance of H/D scrambling allows discarding the formation of cyclopropane intermediates and further ring-opening involving the exchange with water, since the presence of deuterium in the final product cannot be explained through that pathway. Experiments with indole and added D_2O did not provide useful information since blank experiments in the absence of the diazo reagent demonstrated that the catalyst promotes the incorporation of some deuterium into N–H and C3–H.

In view of the lack of decisive support for a mechanistic proposal, we decided to perform DFT studies to ascertain the mechanism governing this transformation.

DFT studies. We have explored the reaction between the metallocarbene complex $[\text{Cu}(\text{ADAP})(\text{CCO}_2\text{EtPh})]^+$ (**i1**) and indole with computational studies and microkinetic simulations.^[12] A dataset of all computational results is available in the ioChem-BD repository,^[13] accessible via <https://doi.org/10.19061/iochem-bd-1-285>.

The absence of cyclopropane intermediates, observed with other catalytic systems, was the first target of this study. We checked the reaction path leading to the cyclopropane intermediate **i4a**, with the free energy profile shown in Figure 2a. The reaction proceeds smoothly with a barrier of $12.7 \text{ kcal}\cdot\text{mol}^{-1}$. This mechanism was the one previously proposed for the Tp^xCu -based catalyst, and does not reproduce the current experimental results. The explanation is in the alternative mechanism indicated in Figure 2b. The two mechanisms share the same path until intermediate **i3a**, where the first carbon-carbon bond is made. A rotational isomer of **i3a**, labeled as **i3**, connects with the transition state **TS 3–4**, which has an associated activation energy of only $7.5 \text{ kcal}\cdot\text{mol}^{-1}$. This step involves an intramolecular proton transfer from the C3 position of the indole to the carbonyl oxygen atom of the PhEDA fragment leading to the metal-associated enol intermediate **i4**. The path in Figure 2b is preferred by nearly $5 \text{ kcal}\cdot\text{mol}^{-1}$, and is thus the favored one, explained the absence of cyclopropane derivatives in



Scheme 6. (a) Previously proposed formation of 3-substituted indoles from cyclopropane intermediates. (b) Use of deuterated indole at C3 **1b-D**.

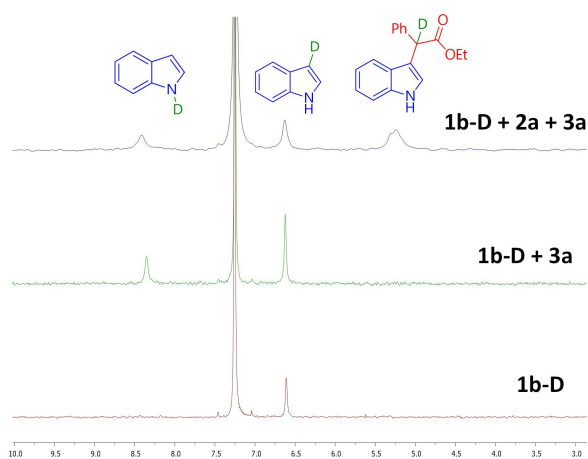


Figure 1. ^2D NMR spectra of (top) the catalytic experiment shown in Scheme 5c; (middle) blank experiment with the **1b-D** indole and the copper catalyst **3a** and (bottom) the indole **1b-D**.

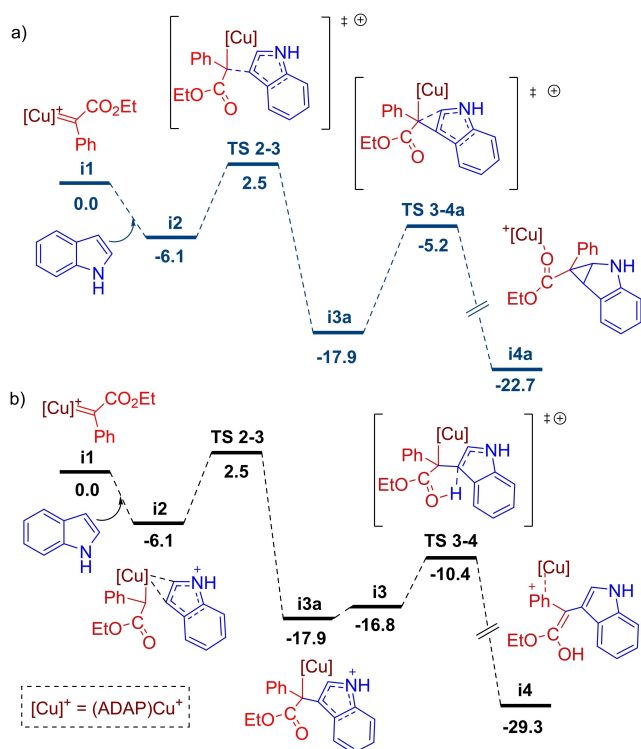


Figure 2. Computed reaction energy profile from DFT calculations with method I for the generation of a) the cyclopropane intermediate and b) the enol intermediate.

the mixture. Efforts to functionalize indoles have been reported with Rh- and Fe-based catalysts which bear similarities to the proposed mechanism.^[14] We notice here that the enolate pathway reported before^[14c], albeit reasonable, has a barrier of 16.1 kcal·mol⁻¹, significantly higher than the one reported here (7.5 kcal·mol⁻¹).

The existence of the two paths with relatively close barriers depicted in Figure 2 raises the question of what happened with the previously reported Tp^{Br}3Cu core.^[8b] Additional calculations reported in the Supporting Information confirmed that there is a preference for the cyclopropane path when the former work conditions are employed. For the sake of completion, we explored a further alternative mechanism leading directly from intermediate **i3** to the reaction product through a [1,2]-H shift. This was found to have a much higher barrier of 32.9 kcal·mol⁻¹ and was thus discarded.

The formation of the enol intermediate **i4**, which resembles that reported by Fasan for myoglobin-catalyzed C3–H functionalization,^[10a] provides a satisfactory explanation for the absence of cyclopropane intermediates, but its conversion into the product is not obvious, and we still need to explain the scrambling of the deuterium mark in the experiment. We thus explored the continuation of the reaction. The dissoci-

ation of the (ADAP)Cu core implies an energy of 24.8 kcal·mol⁻¹; thus the catalyst has to remain attached throughout the reaction. We did compute a metal-free enol pathway, reported in the Supporting Information, because it is simpler and has important indications for the reaction in presence of the catalyst. There are two competitive paths with barriers around 17 kcal·mol⁻¹ above the metal-free enol, which as mentioned above is already more than 20 kcal·mol⁻¹ above the copper complex.

As steps with inclusion of two cationic metal fragments had to be considered, we had to include explicitly the BA^F₄⁻ counteranion to neutralize the system, thus considering **i4BAR**^F₄. If we did not include the counterion, the approach between the two cationic complexes would be artificially penalized by the model simplification. We also had to carry out a small conformational search to find the preferred positions of the BA^F₄⁻ anions. Because of the large number of atoms, the optimization in the calculations that follow was carried out with computational method II. A direct intramolecular [1,3]-H shift within the enol **i4BAR**^F₄ is energetically disfavoured unless there is a proton transfer catalyst, such as water or alcohol.^[15] Figure 3 shows the two catalysed pathways that can arise in the reaction media starting from **i4BAR**^F₄: the dimerization of two enol complexes **i5_{enol}** (black path), where the enol groups act as proton shuttles for each other, and the interaction with a cluster of water molecules **i5_{H2O}** that acts as a proton shuttle (blue path). In the black route of Figure 3, the reaction coordinate in the TS is centered in the transfer of the first proton, the second one follows without forming an intermediate. Details are supplied in the Supporting Information. In the blue route of Figure 3, the [1,3]-H shift is achieved with adventitious H₂O acting as a proton shuttle, as shown in the 3D structure in Figure 4b. We used a water trimer for this calculation, which we found was most efficient in a benchmarking reported in the Supporting Information. At the end of this process, the **2b** product is obtained, lacking, in principle, deuterium marks.

Alternatively, in the black profile of Figure 3, the **i4BAR**^F₄ may interact with another **i4BAR**^F₄, which produces **i5_{enol}**. At **TS 5–6_{enol}** (Figure 4a) both enol complexes act as proton donors and acceptors, giving rise to the **i6_{enol}** product. Consequently, if the reactant is indole **1b-D**, this route would end up with product **2b-D**.

An initial inspection of Figure 3 suggests that the water path should kinetically outperform the enol path. However, the concentration of the reactants in the different processes plays a crucial role.

To evaluate the reproduction of the experimental outcome (40:60 of **2b** and **2b-D**), a microkinetic modeling was carried out (see details in the Supporting Information). It is noteworthy that the cluster of water molecules that transfers a proton to obtain **2b** also

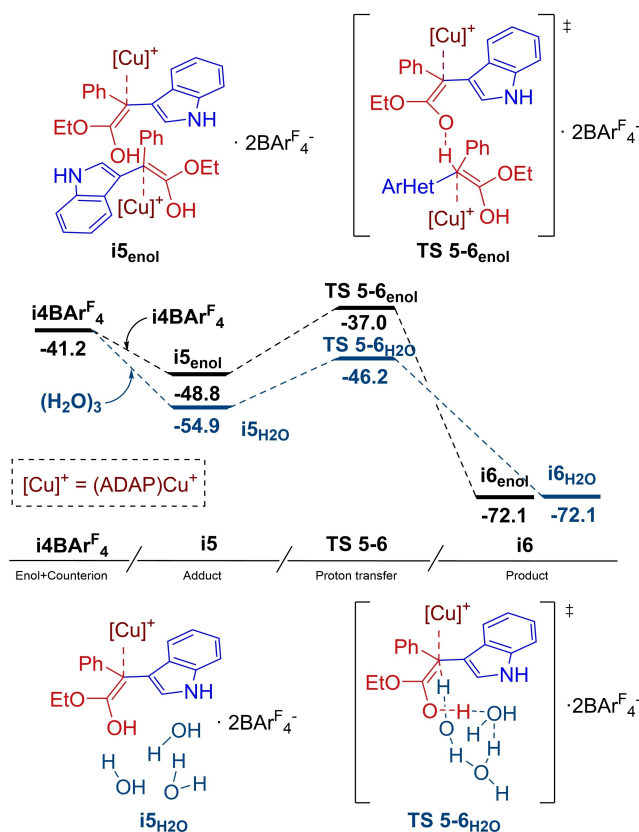


Figure 3. Computed reaction energy profile from DFT calculations with method II for the competitive pathways: the black route is the enol-assisted proton transfer and the blue profile is the water-assisted proton transfer step.

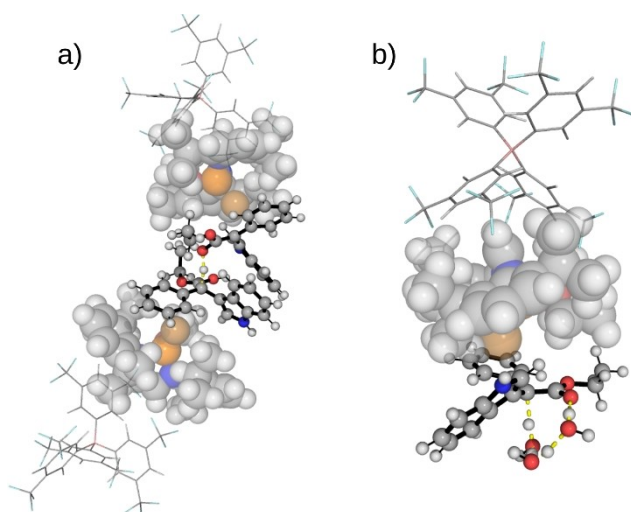


Figure 4. 3D structures of transition states a) TS 5–6_{enol} and b) TS 5–6_{H₂O}. Lines show the BARF₄[–] counteranions, sphere refers to the ADAP-based catalysts and ball and sticks show the rest of the complex.

provides a deuterated cluster. Consequently, an additional competitive pathway, involving TS 5–6_{D₂O}, should be considered. It has been observed that depending on the concentration of water impurities, each pathway dominates the overall mechanism. The experimental findings were successfully replicated with a water concentration [H₂O] of 36 mM.

Therefore, in the deuteration experiments, product **2b** is produced by the water-assisted proton transfer (blue path in Figure 3), whereas the functionalized indole **2b-D** is the product of either the deuterated water acting as a D-shuttle or the dimerization of i4BARF₄ intermediates (black path in Figure 3).

Conclusions

The selective functionalization of the C3–H bond of unprotected indoles has been achieved by means of the copper-catalyzed formal donor-acceptor carbene insertion from diazo compounds. No functionalization of the more reactive N–H bond has been observed. Cyclopropane intermediates have not been detected, at variance with previous work with other Cu-based catalysts. DFT studies indicate that the mechanism differs from previous work done with Tp^{Br3}Cu core. The higher energy barrier of the cyclopropanation respect to the intramolecular proton transfer results in the formation of an enol intermediate. The functionalized product is the result of two competitive pathways using different proton shuttles.

Experimental Section

All reactions and manipulations were carried out under a nitrogen atmosphere by using standard Schlenk techniques or under nitrogen atmosphere in an MBRAUN glovebox. All substrates were purchased from Merck and used without further purification, PhEDA was prepared according to literature methods. Solvents were distilled and degassed before use. NMR spectra were recorded on Agilent 400 MR or Agilent 500 DD2. FTIR spectra were recorded on a Nicolet IR200 FTIR spectrometer. ¹H and ¹³C NMR shifts were measured relative to deuterated solvents peaks but are reported relative to tetramethylsilane. High Resolution Mass Spectroscopy (HRMS) experiments were carried out at the Centre of Research Technology and Innovation of the University of Seville (CITIUS).

General catalytic experiment. The copper complex (0.025 mmol), NaBARF₄ (0.025 mmol), the indole (0.7 mmol) and 4 mL of DCM were added to a Schlenk tube. The diazocompound (0.5 mmol) was added portionwise (one portion every 30 minutes for 3.5 hours). The resulting mixture was stirred at room temperature for 12 h. After this time solvent was removed by reduced pressure and the product was purified by flash chromatography on silica gel 7/1 petroleum/Et₂O with 1% Et₃N.

Computational Details. Calculations were performed at the DFT level using the Gaussian 16 suite of programs.^[16] The

pyssian library^[17] was used for the generation and processing of input and output files. Most calculations were carried out at a full QM description with the ω B97X-D functional.^[18] The 6–31G(d) basis set was^[19] applied for C, H, O, N, B, and F, to all the geometry optimizations and frequency calculations. The Cu atom was described by using the effective core potential (ECP) LANL2DZ^[20] and its associated basis set. An additional f-polarization shell^[21] was added for Cu with an exponent of 3.252. Then, a larger basis sets was used for refining potential energies. The cc-pVTZ basis set^[22] was used for all atoms including Cu, which had again an additional f-polarization shell with the exponent of 3.252. Solvent (dichloromethane, $\epsilon=8.93$) was considered in all QM calculations using the PCM model.^[23] We employed the GoodVibes 3.0.2 program^[24] to perform a Grimme-type^[25] quasi-harmonic correction with a cut-off of 100 cm⁻¹ in the thermochemistry contribution, and we added this entropic term to the QM energy. Some of the calculations for the largest systems used geometry optimizations at the ONIOM(ω B97X-D:UFF)^[26] multilayer scheme. The full description of these ONIOM calculations is indicated in the Supporting Information.

A reference state correction from gas phase (standard concentration at 298 K at 1 atm) to solution phase (1 mol/L) was applied to all the Gibbs energies reported. All the energies reported in the manuscript are Gibbs energies in kcal/mol referred to the metallocarbene (unless stated otherwise).

Acknowledgements

We thank to Ministerio de Ciencia e Innovación for Grants PID2020-113797RB-C21, PID2020-112825RB-I00 and CEX2019-000925-S. We also thank Junta de Andalucía (P18-1536) and Universidad de Huelva (P. O.Feder UHU-202024). I.-G. F thanks the Investigo Program for a contract. L. M.-G. thanks Generalitat de Catalunya for an FI-Agaur predoctoral contract, 2022FI-B2000621.

References



- [1] a) M. P. Doyle, M. A. McKervey, T. Ye, *Modern Catalytic Methods for Organic Synthesis with Diazo Compounds*, Wiley, New York, 1998; b) M. P. Doyle, R. Duffy, M. Ratnikov, L. Zhou, *Chem. Rev.* **2010**, *110*, 704–724.
- [2] Y. He, Z. Huang, K. Wu, J. Ma, Y.-G. Zhou, Z. Yu, *Chem. Soc. Rev.* **2022**, *51*, 2759–2852.
- [3] K. Urbina, D. Tresp, K. Sipps, M. Szostak, *Adv. Synth. Catal.* **2021**, *363*, 2723–2739.
- [4] a) P. M. Dewick, in *Medicinal Natural Products: A Biosynthetic Approach*, Wiley, Chichester, **2009**; b) D. H. R. Barton, K. Nakanishi, O. Meth-Cohn, J. W. Kelly, *Comprehensive Natural Products Chemistry*, Pergamon Press, Oxford, **1999**; c) R. J. Sundberg, *Indoles*, Academic Press, New York, **1996**; d) R. J. Sundberg, *The Chemistry of Indoles*, Academic Press, New York, **1970**; e) A. J. Kochanowska-Karamyan, M. T. Hamann, *Chem. Rev.* **2010**, *110*, 4489–4497; f) S. E. O'Connor, J. J. Maresh, *Nat. Prod. Rep.* **2006**, *23*, 532–547; g) J. Wencel-Delord, F. Glorius Nat, *Chem.* **2013**, *5*, 369–375; h) Y. Y. Xiang, C. Wang, Q. P. Ding, Y. Y. Peng, *Adv. Synth. Catal.* **2019**, *361*, 919–944; i) H. M. L. Davies, J. E. Spangler, in *Advances in Heterocyclic Chemistry*, ed. A. R. Katritzky, Elsevier Academic Press, San Diego, **2013**, vol 110, pp. 43–72.
- [5] a) W. J. Welstead Jr., H. F. Stauffer Jr., L. F. Sancilio, *J. Med. Chem.* **1974**, *17*, 544–547; b) E. Wenkert, M. E. Alonso, H. E. Gottlieb, E. L. Sanchez, *J. Org. Chem.* **1977**, *42*, 3945–3949; c) H. Keller, E. Langer, H. Lehner, *Monatsh. Chem.* **1977**, *108*, 123–131; d) F. Gnad, M. Poleschak, O. Reiser, *Tetrahedron Lett.* **2004**, *45*, 4277–4280; e) S. J. Hedley, D. L. Ventura, P. M. Dominiak, C. L. Nygren, H. M. L. Davies, *J. Org. Chem.* **2006**, *71*, 5349–5356; f) X. J. Zhang, S. P. Liu, M. Yan, *Chin. J. Chem.* **2008**, *26*, 716–720; g) P. K. Dutta, J. Chauhan, M. K. Ravva, S. Sen, *Org. Lett.* **2019**, *21*, 2025–2028; h) G. Özüdüru, T. Schubach, M. M. K. Boysen, *Org. Lett.* **2012**, *14*, 4990–4993; i) Z. Wang, G. Xu, S. Tang, Y. Shao, J. Sun, *Org. Lett.* **2019**, *21*, 8488–8491.
- [6] a) R. Gibe, M. A. Kerr, *J. Org. Chem.* **2002**, *67*, 6247–6249; b) V. Arredondo, S. C. Hiew, E. S. Gutman, I. D. U. A. Premachandra, D. L. Van Vranken, *Angew. Chem. Int. Ed.* **2017**, *56*, 4156–4159.
- [7] W. W. Chan, S. H. Yeung, Z. Zhou, A. S. C. Chan, W. Y. Yu, *Org. Lett.* **2010**, *12*, 604–607.
- [8] a) R. Give, M. A. Kerr, *J. Org. Chem.* **2002**, *67*, 6247–6249; b) M. Delgado-Rebollo, A. Prieto, P. J. Pérez, *ChemCatChem.* **2014**, *6*, 2047–2052; c) Y. Yang, Z. Shi, *Chem. Commun.* **2018**, *54*, 1676–1685; d) S. Muthusamy, C. Gunanathan, S. A. Babu, E. Suresh, P. Dastidar, *Chem. Commun.* **2002**, *8*, 824–825; e) S. Muthusamy, B. Gnanaprakasam, *Tetrahedron Lett.* **2008**, *49*, 475–480; f) A. DeAngelis, V. W. Shurtleff, O. Dmitrenko, J. M. Fox, *J. Am. Chem. Soc.* **2011**, *133*, 1650–1653; g) T. Goto, Y. Natori, K. Takeda, H. Nambu, S. Hashimoto, *Tetrahedron: Asymmetry* **2011**, *22*, 907–915; h) Y. Lian, H. M. L. Davies, *Org. Lett.* **2012**, *14*, 1934–1937; i) Y. Cai, S. F. Zhu, G. P. Wang, Q. L. Zhou, *Adv. Synth. Catal.* **2011**, *353*, 2939–2944; j) X. Gao, B. Wu, W. X. Huang, M. W. Chen, Y. G. Zhou, *Angew. Chem. Int. Ed.* **2015**, *54*, 11956–11960; k) K. Liu, G. Xu, J. Sun, *Chem. Sci.* **2017**, *9*, 634–639.
- [9] a) K. H. Hock, A. Knorrscheidt, R. Hommelsheim, J. Ho, M. J. Weissenborn, R. M. Koenigs, *Angew. Chem. Int. Ed.* **2019**, *58*, 3630–3634; b) S. Jana, C. Empel, C. Pei, P. Aseeva, T. V. Nguyen, R. M. Koenigs, *ACS Catal.* **2020**, *10*, 9925–9931.
- [10] a) D. A. Vargas, A. Tinoco, V. Tyagi, R. Fasan, *Angew. Chem. Int. Ed.* **2018**, *57*, 9911–9915; b) O. F. Brandenburg, K. Chen, F. H. Arnold, *J. Am. Chem. Soc.* **2019**, *141*, 8989–8995.
- [11] J. D. Pizarro, F. Molina, M. R. Fructos, P. J. Pérez, *Chem. Eur. J.* **2020**, *26*, 10330–10335.
- [12] a) M. Besora, F. Maseras, *WIREs Comput. Mol. Sci.* **2018**, *8*, e1372; b) R. Pérez-Soto, M. Besora, F. Maseras, *Org. Lett.* **2020**, *22*, 2873–2877.

- [13] M. Álvarez-Moreno, C. de Graaf, N. López, F. Maseras, J. M. Poblet, C. Bo, *Chem. Inf. Model.* **2015**, *55*, 95–103.
- [14] a) A. DeAngelis, V. W. Shurtleff, O. Dmitrenko, J. M. Fox, *J. Am. Chem. Soc.* **2011**, *133*, 1650–1653; b) Q. Xie, X. S. Song, D. Qu, L. P. Guo, Z. Z. Xie, *Organometallics* **2015**, *34*, 3112–3119; c) R. Balhara, G. Jindal, *J. Org. Chem.* **2022**, *12*, 7919–7933.
- [15] a) Y. Xia, Y. Liang, Y. Chen, M. Wang, L. Jiao, F. Huang, S. Liu, Y. Li, Z. X. Yu, *J. Am. Chem. Soc.* **2007**, *129*, 3470–3471; b) S. -S. Meng, Y. Liang, K. -S. Cao, L. Zou, X. -B. Lin, H. Yang, K. N. Houk, W. -H. Zheng, *J. Am. Chem. Soc.* **2014**, *136*, 12249–12252.
- [16] M. J. Frisch, G. W. Trucks, H. B. Schlegel, G. E. Scuseria, M. A. Robb, J. R. Cheeseman, G. Scalmani, V. Barone, G. A. Petersson, H. Nakatsuji, X. Li, M. Caricato, A. V. Marenich, J. Bloino, B. G. Janesko, R. Gomperts, B. Mennucci, H. P. Hratchian, J. V. Ortiz, A. F. Izmaylov, J. L. Sonnenberg, D. Williams-Young, F. Ding, F. Lipparini, F. Egidi, J. Goings, B. Peng, A. Petrone, T. Henderson, D. Ranasinghe, V. G. Zakrzewski, J. Gao, N. Rega, G. Zheng, W. Liang, M. Hada, M. Ehara, K. Toyota, R. Fukuda, J. Hasegawa, M. Ishida, T. Nakajima, Y. Honda, O. Kitao, H. Nakai, T. Vreven, K. Throssell, J. A. Montgomery, Jr., J. E. Peralta, F. Ogliaro, M. J. Bearpark, J. J. Heyd, E. N. Brothers, K. N. Kudin, V. N. Staroverov, T. A. Keith, R. Kobayashi, J. Normand, K. Raghavachari, A. P. Rendell, J. C. Burant, S. S. Iyengar, J. Tomasi, M. Cossi, J. M. Millam, M. Klene, C. Adamo, R. Cammi, J. W. Ochterski, R. L. Martin, K. Morokuma, O. Farkas, J. B. Foresman, D. J. Fox, Gaussian 16 Revision C.01.
- [17] R. Pérez-Soto, M. Besora, F. Maseras, Pyssian v1.0.2; Maseras Lab. July 1, **2021**.
- [18] J. -D. Chai, M. Head-Gordon, *Phys. Chem. Chem. Phys.* **2008**, *10*, 6615–6620.
- [19] a) M. M. Francl, W. J. Pietro, W. J. Hehre, J. S. Binkley, M. S. Gordon, D. J. DeFrees, J. A. Pople, *J. Chem. Phys.* **1982**, *77*, 3654; b) P. C. Hariharan, J. A. Pople, *Theor. Chim. Acta* **1973**, *28*, 213; c) W. J. Hehre, R. Ditchfield, J. A. Pople, *J. Chem. Phys.* **1972**, *56*, 2257.
- [20] P. J. Hay, W. R. Wadt, *J. Chem. Phys.* **1985**, *82*, 270–283.
- [21] A. W. Ehlers, M. Böhme, S. Dapprich, A. Gobbi, A. Höllwarth, V. Jonas, K. F. Köhler, R. Stegmann, A. Veldkamp, G. Frenking, *Chem. Phys. Lett.* **1993**, *208*, 111.
- [22] D. E. Woon, T. H. Dunning, Jr., *J. Chem. Phys.* **1993**, *98*, 1358–1371.
- [23] J. Tomasi, B. Mennucci, R. Cammi, *Chem. Rev.* **2005**, *105*, 2999–3094.
- [24] G. Luchini, J. Alegre-Requena, I. Funes, J. Rodríguez-Guerra, J. T. Chen, R. Paton, Bobbypaton/GoodVibes: GoodVibes v3.0.2. **2019**. <https://doi.org/10.5281/ZENODO.3346166>.
- [25] S. Grimme, *Chem. A Eur. J.* **2012**, *18*, 9955–9964.
- [26] F. Maseras, K. Morokuma, *J. Comput. Chem.* **1995**, *16*, 1170–1179.

RESEARCH ARTICLE

Selective C–H Bond Functionalization of Unprotected Indoles by Donor-Acceptor Carbene Insertion

Adv. Synth. Catal. **2023**, *365*, 1–9

 J. Diego Pizarro, L. Morán-González, I. González-Fernández,
 F. Maseras*, M. R. Fructos*, P. J. Pérez*

